

From (C5) and (C6) it follows that

$$\begin{aligned} \mathcal{D}_{00}^{(2)}(\Omega_i') &\equiv f(\chi, \theta, \phi) \\ &= (1 - 3 \sin^2 \theta + (9/4) \sin^4 \theta) \\ &\quad + 3 \sin^2 \theta \cos^2 \theta \cos \chi + \frac{3}{4} \sin^4 \theta \cos 2\chi. \quad (C7) \end{aligned}$$

Hence, if the average in (C4) is expressed in terms of

the angles  $(\chi, \theta, \phi)$ , one obtains

$$\begin{aligned} &\langle [\mathcal{D}_{0l'}^{(2)}(\Omega_i)]_{t+\tau} [\mathcal{D}_{0k'}^{(2)}(\Omega_i)]_t \rangle \\ &= (\frac{1}{5}) \delta_{-l', k'} (-1)^{k'} \int_0^{2\pi} \int_0^\pi \int_0^\pi f(\chi, \theta, \phi) F(\chi) \\ &\quad \times \sin \theta d\chi d\theta d\phi, \quad (C8) \end{aligned}$$

where  $F(\chi)$  is given by (5.14). The integrals in (C8) can be easily performed to obtain the result given by Eq. (5.16).

## L-Shell Fluorescence Yields in Heavy Elements\*

R. C. JOPSON, HANS MARK, C. D. SWIFT, AND M. A. WILLIAMSON  
*Lawrence Radiation Laboratory, University of California, Livermore, California*  
 (Received 29 March 1963)

Partial  $L$ -shell fluorescence yields of 23 heavy elements have been measured using an x-ray coincidence counting method. Vacancies in the  $K$  shell of the target atoms are created by photoelectric absorption of 122- and 136-keV gamma rays emitted by a  $\text{Co}^{57}$  source. A known fraction of these  $K$ -shell vacancies are filled by  $L$  electrons. The  $L$ -shell vacancies created in this way are then occupied by electrons from higher shells, causing emission of  $L$  x rays and Auger electrons. The coincidence rate between the  $L$  and  $K$  x rays determines the fluorescence yield  $\omega_{KL}$ , which is defined as the partial  $L$ -shell fluorescence yield following the emission of  $K_\alpha$  x rays.  $\omega_{KL}$  is a linear combination of the fluorescence yields of the  $L_{II}$  and  $L_{III}$  subshells. A comprehensive comparison with previous measurements is given.

### INTRODUCTION

IN a previous article,<sup>1</sup> a method of measuring fluorescence yields of the  $L$  shell of heavy elements was described. Vacancies are created in the  $K$  shell of an atom and the coincidence rate between the  $K$  and  $L$  x rays emitted subsequent to the ionization event is determined. This coincidence rate depends upon the partial  $L$ -shell fluorescence yield  $\omega_{KL}$ , defined in Ref. 1 in the following way:

$$\omega_{KL} = \frac{N_c}{N_K} \frac{1}{a E_L A_L \Omega_L}. \quad (1)$$

In Eq. (1),  $N_c$  is the  $L$  to  $K$  x-ray coincidence rate,  $N_K$  the  $K$  x-ray counting rate,  $\Omega_L$  the geometry of the  $L$  x-ray counter, and  $E_L$  the efficiency of the  $L$  x-ray counter. The quantity  $A_L$  is the transmission of  $L$  x rays to the  $L$  x-ray counter, and  $a$  is the fraction of counts in  $K$  x-ray peak due to  $K_{\alpha_2}$  and  $K_{\alpha_1}$  x rays. The last factor  $a$  must be included since the  $K$  x-ray counter cannot resolve those  $K$  x rays ( $K_\alpha$  lines) which leave a vacancy in the  $L$  shell from those which do not ( $K_\beta$  lines). In the previous work,  $K$ -electron capture or  $K$ -shell internal conversion processes were used to create the  $K$ -shell vacancies. This method cannot be

applied to a large number of elements because most decay schemes are so complex that a unique interpretation of the results is not possible. In the present experiments, the  $K$  shells of the target atoms were ionized by photoelectric absorption. Thin foils of the target material are exposed to gamma rays with a sufficiently high energy to cause  $K$ -shell ionization, and the coincidence rate between the  $K$  and  $L$  x rays emitted by the foil is measured. Therefore, the methods described in Ref. 1 can be extended to a large number of elements.

### EXPERIMENTAL PROCEDURE

The experimental geometry is shown in Fig. 1. A 20-mCi  $\text{Co}^{57}$  source was placed in a carefully shielded source holder. The gamma rays<sup>2</sup> emitted by the source were collimated and directed at the thin target foil ( $\frac{5}{8}$  in.  $\times$   $\frac{5}{8}$  in.) placed between the two counters. The target foil was mounted on the aluminum target holder with very thin (less than 0.001-in. diam) nylon fibers. This was done to minimize the amount of material in the path of the gamma-ray beam in order to reduce the background from Compton scattering. The  $K$  and  $L$  x-ray counters were both similar to those used in the previous experiment. Thin (approximately 0.030 in.) NaI(Tl) crystals were used to detect both the  $L$  and

\* Work done under auspices of the U. S. Atomic Energy Commission.

<sup>1</sup> R. C. Jopson, Hans Mark, and C. D. Swift, Phys. Rev. **128**, 2671 (1962).

<sup>2</sup> D. Strominger, J. M. Hollander, and G. T. Seaborg, Rev. Mod. Phys. **30**, 585 (1958).

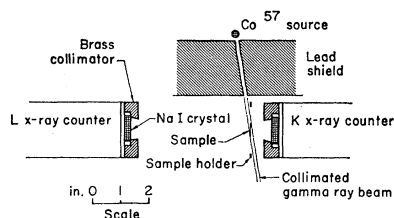


FIG. 1. The experimental arrangement for measuring  $\omega_{KL}$  is shown in this figure. Both counters and source were enclosed in a cooled box not shown in the drawing.

the  $K$  x rays. The crystal used in the  $L$  x-ray counter was cleaved from a block of material and the surface toward the source was not polished. Two-mil-thick (0.002 in.) beryllium windows covered the crystals to make them light-tight and to keep out the moisture. An RCA 6810A photomultiplier tube was used to view the scintillation crystal in the  $K$  x-ray counter, and an EMI 9584S tube was used for the  $L$  x-ray counter. Single-channel pulse-height analyzers were employed to define appropriate electronic windows for the  $K$  and  $L$  x rays in each counter.

The most difficult experimental problem that had to be solved was to produce target foils sufficiently thin and uniform to serve as good x-ray sources. In order to keep the self-absorption of  $L$  x rays in the target foils below approximately 50%, the thickness of the foils was limited to less than 10 mg/cm<sup>2</sup>. In some cases it was possible to obtain pure metal foils which are sufficiently thin. For most of the materials, however, it was necessary to make target foils from finely powdered samples of the oxide of the element. This was done by mixing the powdered material with polystyrene dissolved in benzene. This mixture was then poured on a glass plate and allowed to dry. The thin film produced in this manner was separated from the glass backing and cut to proper size. Target films of this kind were prepared for almost all of the rare-earth oxides used in these experiments. The target thickness in mg/cm<sup>2</sup> was obtained by weighing the foils and then dividing by the area. This procedure was not always correct, as is shown in Table I. Here, the ratios of the coincidence counting rates to the  $K$  x-ray count rates  $(N_c/N_K)c$  (corrected for self-absorption of the  $L$  x rays in the target foil) are shown for a number of different target foils of the same element. It can be seen that the ratios for the powdered oxide targets are uniformly lower than for the metal foils. The reason for this effect is that the powdered targets were sometimes quite grainy (10–50  $\mu$

in diameter) so that weighing the foil is not an accurate way of measuring the thickness. Correction factors (usually of the order of 10%) for the oxide targets were obtained by making appropriate comparisons with neighboring elements where data both for metal foils and oxide targets were available.

With the geometry shown in Fig. 1 and the 20-mCi  $\text{Co}^{57}$  source (4 in. between the foil and the  $L$  x-ray counter), counting rates of the order of 1–10 coincidences per minute and 1000–10 000  $K$  x-ray counts/min were obtained. In order to reduce counting statistics below other errors inherent in the experiment, between 5000 and 10 000 coincidence counts had to be obtained. This meant that fairly long runs were necessary (somewhere between 10 and 100 h) to collect the data for one sample. In order to keep the electronic window positions as stable as possible over such long periods of time, the

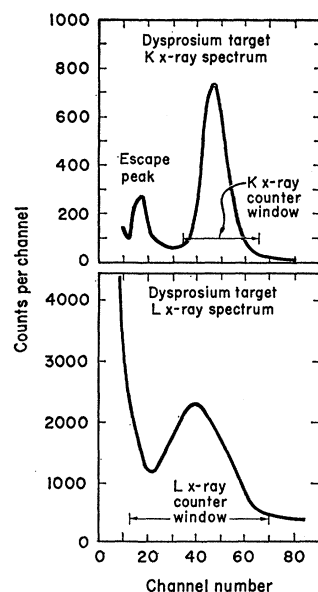


FIG. 2. This drawing shows the  $K$  and  $L$  x-ray spectra observed from a dysprosium target. These spectra are typical of those observed in the rare-earth region.

TABLE I. Comparison between oxide and metal foil targets.

Element	Z	$(N_c/N_K)c$		Ratio, oxide/metal
		Oxide ( $\times 10^{-4}$ )	Metal ( $\times 10^{-4}$ )	
Bismuth	83	6.21	6.85	0.907
Gold	79	5.50	6.04	0.911
Tantalum	73	4.08	4.51	0.905
Holmium	67	2.78	3.35	0.830
Samarium	62	2.01	2.16	0.931

whole system was placed in a temperature-controlled box. The solid angle for the  $L$  counter was computed by assuming that the foil is a point source. This approximation is reasonable since the linear dimension of the foil was much smaller than the distance between the foil and the  $L$  x-ray counter. The  $K$ -counter solid angle was as large as possible in order to increase the counting rate as much as possible. It is not necessary to know what this solid angle is, since it does not appear in the formula for  $\omega_{KL}$ . A typical pulse-height spectrum in the  $K$  and the  $L$  counter of the system is shown in Fig. 2. The counter window widths are also indicated in the figure. Care must be taken that all the  $L$  x rays are included in the window, since it is tacitly assumed in Eq. (1) that all  $L$  x rays are observed. The  $L$  x-ray window shown in Fig. 2 includes some phototube noise. This does not affect the value of  $\omega_{KL}$  given in Eq. (1),

but it does increase the random counts which must be subtracted from the measured coincidence counts.

A number of effects had to be considered in order to compute appropriate background corrections for  $N_c$  (the coincidence rate) and  $N_K$  (the  $K$  x-ray counting rate). A background count in each counter and also in the coincidence channel was measured with no target holder in place for each run. This measurement determines the background caused by cosmic rays and stray radiation near the counters. In addition, another background measurement for each run was made with a 10.8-mg/cm<sup>2</sup> Cu foil mounted in the target holder. This target is designed to simulate all those counts caused by events in the real target other than  $K$ -shell ionization. These include Compton scattering, photoelectric emission of electrons other than those in the  $K$  shell, and a number of smaller effects. In a typical case, the experimentally determined background rate in the  $K$  x-ray counter was of the order of 10%. The coincidence background measured in this manner was usually of the order of 3%, and the random coincidence rate was also approximately 3%.

Table II shows some typical numbers used in the calculation of  $\omega_{KL}$  for a representative sample of elements. The ratios  $N_c/N_K$  are shown in column 3. The fourth column shows the thickness in mg/cm<sup>2</sup> and the target material, and the fifth column shows the transmission factor  $A_L$  for each of the targets. The geometrical factor  $\Omega_L$  is almost the same for each of the runs, and the efficiency factor  $E_L$  for all the  $L$  x rays is assumed to be unity. The estimated standard errors in the values of  $\omega_{KL}$  are primarily due to errors in computing  $A_L$ , errors in estimating the geometry of the  $L$  x-ray counter, and counting statistics. The geometry is known to  $\pm 2\%$ , and the counting statistics are also about  $\pm 2\%$ . The most difficult error to estimate is in the transmission factor  $A_L$ . This quantity is the product of three factors, the fraction of  $L$  x rays transmitted through the target foil, the fraction transmitted through the air between the target foil and the counter, and the fraction transmitted by the beryllium window of the counter. To obtain reasonable estimates

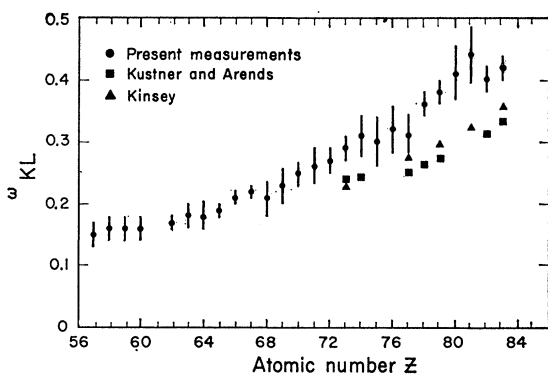


FIG. 3. The present results are summarized in this drawing. Earlier numbers for selected elements are also shown for comparison.

TABLE II. Examples of some typical coincidence to  $K$  x-ray ratios and  $L$  x-ray transmission factors.

Element	Z	$N_c/N_K$	Target	$A_L$
Lanthanum	57	$7.75 \times 10^{-5}$	La <sub>2</sub> O <sub>3</sub> target (5.04) <sup>a</sup> Polystyrene backing (0.87)	0.296
Neodymium	60	$1.20 \times 10^{-4}$	Nd <sub>2</sub> O <sub>3</sub> target (3.95) Polystyrene backing (2.5)	0.462
Dysprosium	66	$1.70 \times 10^{-4}$	Dy <sub>2</sub> O <sub>3</sub> target (4.85) Polystyrene backing (1.9)	0.556
Tantalum	73	$2.45 \times 10^{-4}$	Ta metal foil (10.0)	0.487
Gold	79	$5.19 \times 10^{-4}$	Au metal foil (2.70)	0.809
Bismuth	83	$5.53 \times 10^{-4}$	Bi metal foil (4.46)	0.780

<sup>a</sup> Numbers in parentheses are target thicknesses, expressed in mg/cm<sup>2</sup>.

of the air and beryllium window transmission, it was necessary to compute an average energy for the  $L$  x rays. It was, therefore, necessary to estimate the relative intensities of each of the five major components ( $L_{\alpha_2}$ ,  $L_{\alpha_1}$ ,  $L_{\beta_1}$ ,  $L_{\beta_2}$ , and  $L_{\gamma_1}$ ) of the  $L$  x-ray line. This has been done, using the theoretical relative intensity<sup>3</sup> for each of the two multiplets ( $L_{\alpha_1}:L_{\alpha_2}:L_{\beta_1}=9:1:5$  and  $L_{\beta_2}:L_{\gamma_1}=9:5$ ) and then using an experimentally measured number<sup>4</sup> to obtain the relative intensities of the two multiplets. A slightly more complicated procedure was used in the case of "self-transmission" of the foil. Absorption coefficients near the  $L$  edges of the target materials had to be estimated from the available measurements on Pb, Tl, Pt, W, and Ag.<sup>5</sup> Since many of the target materials have atomic numbers between 74 (W) and 47 (Ag), large extrapolations were necessary which introduce correspondingly large errors. The absorption coefficients for air and beryllium were taken from NBS Circular No. 583.<sup>6</sup> The largest errors occur in the case of the lowest  $Z$  materials because, for these, as many as three-quarters of the  $L$  x rays produced in the target foil may be absorbed in one way or another before they reach the  $L$  x-ray counter. The behavior of  $\omega_{KL}$  as a function of atomic number ( $Z$ ) is shown in Fig. 3.

## DISCUSSION OF RESULTS

The values obtained for  $\omega_{KL}$  in the course of the present work are listed in Table III. Previous measurements of  $L$ -shell fluorescence yields are also shown in this table. Great care must be taken when comparisons of this kind are made because each experiment usually determines a slightly different "partial" or "average" fluorescence yield of the  $L$  shell. The fluorescence yield of an atomic shell or subshell  $\omega_{LX}$  is defined as the ratio of the number of x rays emitted in single transitions to the shell or subshell to the number of holes

<sup>3</sup> H. E. White and A. Y. Eliason, Phys. Rev. **44**, 753 (1933).

<sup>4</sup> A. H. Compton and S. K. Allison, *X Rays in Theory and Experiment* (D. Van Nostrand, Inc., New York, 1934).

<sup>6</sup> Rosemary T. McGinnies, Suppl. NBS Circular No. 583, 1959 (unpublished).

created in the shell or subshell. The  $L$  shell consists of three subshells  $L_I(s_{1/2})$ ,  $L_{II}(p_{1/2})$ , and  $L_{III}(p_{3/2})$ . Since the fluorescence yield of each of the  $L$  subshells is different, the average  $L$ -shell yield measured will depend on the number of holes created in each of the shells. The "average  $L$ -shell fluorescence yields" defined by a number of different experimenters therefore depends upon how the  $L$  shell was ionized. The situation is further complicated by the existence of Coster-Kronig transitions.<sup>6</sup> In these transitions, a hole created in the  $L_I$  shell may be filled by an electron from the  $L_{II}$  or  $L_{III}$  shell, accompanied by the emission of an Auger electron from one of the higher atomic shells. A certain fraction of the holes created in the  $L_I$  shell are thus filled by  $L_{II}$  or  $L_{III}$  electrons, causing holes in the  $L_{II}$  or  $L_{III}$  shell. Thus, not all the holes in the  $L_{II}$  or  $L_{III}$  shell are caused by direct ionization of that shell, and this effect must be taken into account when the average fluorescence yield is computed. In the following discussion, the definitions and notations given by Wapstra, Nijgh, and van Lieshout<sup>7</sup> will be used.

The average  $L$ -shell fluorescence yield is given by

$$\bar{\omega}_L = N_{L_I} \nu_{L_I} + N_{L_{II}} \nu_{L_{II}} + N_{L_{III}} \nu_{L_{III}}, \quad (2)$$

where  $N_{L_I}$ ,  $N_{L_{II}}$ , and  $N_{L_{III}}$  are the fractions of primary vacancies produced in the  $L_I$ ,  $L_{II}$ , and  $L_{III}$  subshells. The quantity  $\nu_{L_X}$  is defined as the number of  $L$  x rays emitted divided by the number of vacancies in the  $L_X$  shell. This quantity differs from  $\omega_{L_X}$  in that the  $L$  x ray is not required to come from a transition to the  $L_X$  shell. It is, thus, possible to treat Coster-Kronig transitions in a relatively simple way. In the case of the  $L$  shell, the important Coster-Kronig transitions in the region between  $Z=57$  and  $Z=82$  are those in which holes in the  $L_I$  shell are transferred either to the  $L_{II}$  shell, producing Auger electrons from the  $N$  shell [ $L_I \rightarrow L_{II}(N)$ ], or to the  $L_{III}$  shell, producing Auger electrons from the  $M$  shell [ $L_I \rightarrow L_{III}(M)$ ]. The latter transitions are energetically possible only for  $Z > 73$ ; however, they have a higher probability of occurring because  $M$  electrons are closer to the  $L$  shell than are the  $N$  electrons, thereby increasing the wave function overlap in the matrix element of the transitions. Coster-Kronig transitions between  $L_{II}$  and the  $L_{III}$  shell are infrequent enough that they can be neglected.

The quantities  $\nu_{L_X}$  can now be expressed in terms of the  $\omega_{L_X}$ 's as follows:

$$\begin{aligned} \nu_{L_{III}} &= \omega_{L_{III}}, \\ \nu_{L_{II}} &= \omega_{L_{II}}, \\ \nu_{L_I} &= \omega_{L_I} + f_{L_I L_{II}} \omega_{L_{II}} + f_{L_I L_{III}} \omega_{L_{III}}, \end{aligned} \quad (3)$$

where  $f_{L_I L_{II}}$  and  $f_{L_I L_{III}}$  are the appropriate Coster-Kronig transition probabilities.

<sup>6</sup> D. Coster and R. Kronig, *Physica* 2, 13 (1935).

<sup>7</sup> A. H. Wapstra, G. J. Nijgh, and R. van Lieshout, *Nuclear Spectroscopy Tables* (North-Holland Publishing Company, Amsterdam, 1959).

TABLE III. Summary of experimental results.

Element	$Z$	$\omega_{KL}$ (Present measurements)	$\omega_{KL}$ (Previous results)	$\bar{\omega}_L$ (Lay, Ref. 14)
Bismuth	83	0.42±0.03	0.44±0.02 <sup>a</sup> 0.33 <sup>b</sup> 0.353 <sup>c</sup>	0.402
Lead	82	0.40±0.02	0.313 <sup>b</sup> 0.314 <sup>d</sup>	0.398
Thallium	81	0.44±0.05	0.38±0.02 <sup>a</sup> 0.322 <sup>c</sup>	...
Mercury	80	0.41±0.05	0.366 <sup>e</sup>	...
Gold	79	0.38±0.02	0.274 <sup>b</sup> 0.304 <sup>d</sup> 0.295 <sup>e</sup>	0.365
Platinum	78	0.36±0.02	0.266 <sup>b</sup> 0.286 <sup>d</sup>	0.348
Iridium	77	0.31±0.04	0.256 <sup>b</sup> 0.277 <sup>c</sup>	...
Osmium	76	0.32±0.04	...	0.348
Rhenium	75	0.30±0.04	...	...
Tungsten	74	0.31±0.04	0.242 <sup>b</sup>	0.298
Tantalum	73	0.29±0.02	0.236 <sup>b</sup> 0.230 <sup>d</sup> 0.233 <sup>e</sup> 0.28±0.01 <sup>f</sup> 0.24±0.01 <sup>f</sup>	...
Hafnium	72	0.27±0.02	...	...
Lutetium	71	0.26±0.03	...	...
Ytterbium	70	0.25±0.02	...	...
Thulium	69	0.23±0.03	...	...
Erbium	68	0.21±0.03	...	0.228
Holmium	67	0.22±0.01	...	...
Dysprosium	66	0.21±0.01	...	...
Terbium	65	0.19±0.01	...	...
Gadolinium	64	0.18±0.02	...	0.198
Europium	63	0.18±0.02	...	...
Samarium	62	0.17±0.01	...	0.188
Neodymium	60	0.16±0.02	...	0.170
Praseodymium	59	0.16±0.02	...	0.167
Cerium	58	0.16±0.02	...	0.163
Lanthanum	57	0.15±0.02	...	0.158

<sup>a</sup> Ref. 1.

<sup>b</sup> Ref. 8.

<sup>c</sup> Ref. 11.

<sup>d</sup> Ref. 9.

<sup>e</sup> Ref. 10.

<sup>f</sup> Ref. 13.

The quantity  $\omega_{KL}$  determined in the present experiments is an "average  $L$ -shell fluorescence yield" given by

$$\omega_{KL} = 0.33 \nu_{L_{II}} + 0.67 \nu_{L_{III}} = 0.33 \omega_{L_{II}} + 0.67 \omega_{L_{III}}. \quad (4)$$

Equation (4) has the same form as Eq. (2). The coefficients of the subshell yields are determined by the ionization process—in this case, the transition of  $L$  electrons to holes in the  $K$  shell. The  $\Delta l = \pm 1$  selection rule forbids the transitions  $L_I \rightarrow K$ , therefore  $N_{L_I}$  vanishes. The values of  $N_{L_{II}}$  and  $N_{L_{III}}$  are obtained, respectively, from the observed intensities of  $K_{\alpha_1}$  and  $K_{\alpha_2}$  x rays, which are caused, respectively, by  $L_{III} \rightarrow K$  and  $L_{II} \rightarrow K$  transitions. These intensities vary slightly from element to element but the 2:1 ratio given in Eq. (4) is a reasonably good approximation.

Two comparisons with previous data can be made. In some instances, the quantities  $\omega_{L_{II}}$  and  $\omega_{L_{III}}$  have been determined independently by a number of different methods so that it is possible to calculate  $\omega_{KL}$  using Eq. (4). In other cases, various experimenters have measured average  $L$ -shell fluorescence yields defined by different values of the coefficients  $N_{L_I}$ ,  $N_{L_{II}}$ , and  $N_{L_{III}}$

in Eq. (2). In the second case, care must be taken that the proper quantities are compared with each other.

Column 4 in Table III shows the values of  $\omega_{KL}$  computed from previous measurements of  $\omega_{LII}$  and  $\omega_{LIII}$ . Measurements of Küstner and Arends,<sup>8</sup> Roos,<sup>9</sup> and Haynes and Achor<sup>10</sup> have been used for this compilation. The values due to Kinsey<sup>11</sup> were obtained by comparing the radiative widths of various x-ray emission lines with the total widths of the appropriate absorption edges. Data from a number of different experiments were used by Kinsey to make the compilation. The salient feature of this comparison is that the present measurements are larger by about 20% than most of the previous data. Important exceptions to this conclusion are the results of Haynes and Achor (for  $Z=80$ ),<sup>10</sup> Risch and others (for  $Z=82$ ),<sup>12</sup> and some previous work of the present authors (for  $Z=73, 74, 81$ , and  $83$ ).<sup>1,13</sup> These values, which are all the result of relatively recent experiments, are all in reasonably good agreement with the present results.

Column 5 in Table III shows the average fluorescence yields ( $\bar{\omega}_L$ ) given by Lay.<sup>14</sup> Lay's measurements of the fluorescent yield were made by using Mo  $K_\alpha$  x rays to ionize the  $L$  shell of the sample material. The fluorescence yield was then obtained by comparing the intensity of the reradiated  $L$  x rays with the primary beam intensity. Photographic plate techniques were used to compare the intensities, and computed theoretical values of the  $L$ -shell absorption coefficients<sup>15</sup> were used to obtain the number of primary  $L$ -shell vacancies from the incident Mo  $K_\alpha$  x-ray intensity. The "average  $L$ -shell fluorescence yield" measured in this manner is

$$\bar{\omega}_L = 0.167\nu_{LI} + 0.333\nu_{LII} + 0.50\nu_{LIII}. \quad (5)$$

<sup>8</sup> H. Küstner and E. Arends, Ann. Phys. (Leipzig) **22**, 443 (1935).

<sup>9</sup> C. E. Roos, quoted in B. L. Robinson and R. W. Fink, Rev. Mod. Phys. **32**, 117 (1960).

<sup>10</sup> S. K. Haynes and W. T. Achor, J. Phys. Radium **16**, 635 (1955).

<sup>11</sup> B. B. Kinsey, Can. J. Res. **A26**, 404 (1948).

<sup>12</sup> K. Risch, Z. Physik **150**, 87 (1958).

<sup>13</sup> R. C. Jopson, H. Mark, C. D. Swift, and J. H. Zenger, Phys. Rev. **124**, 157 (1961).

<sup>14</sup> H. Lay, Z. Physik **91**, 533 (1935).

<sup>15</sup> H. Lay, Z. Physik **91**, 551 (1935).

The coefficients of  $\nu_{LI}$ ,  $\nu_{LII}$ , and  $\nu_{LIII}$  are obtained by using the calculated  $L$ -shell absorption coefficients. There is a  $Z$  dependence which has been neglected for the purpose of the present calculation because it is not very strong. Equation (5) represents a reasonably good approximation of Lay's average fluorescence yield. The difference between  $\omega_L$  and  $\omega_{KL}$  is approximately

$$\Delta\omega = \bar{\omega}_L - \omega_{KL} = 0.167(\nu_{LI} - \nu_{LIII}). \quad (6)$$

The validity of the comparison with Lay's results therefore depends on the relative magnitude of  $\nu_{LI}$  and  $\nu_{LIII}$ . If the difference is small, then  $\bar{\omega}_L \approx \omega_{KL}$ . In the region  $Z > 73$ , Coster-Kronig transitions of the type  $L_I \rightarrow L_{III}(M)$  occur with a large probability so that most of the primary  $L_I$ -shell vacancies are changed to vacancies in the  $L_{III}$  shell. Thus,  $\nu_{LI}$  and  $\nu_{LIII}$  are very nearly the same and  $\Delta\omega$  has values near 0.01 or 0.02. In this region ( $Z > 73$ ), good agreement between  $\bar{\omega}_L$  and  $\omega_{KL}$  should be obtained, which is consistent with the results shown in Table III. For values of  $Z$  less than 73, the Coster-Kronig transition cannot occur and therefore very precise agreement cannot be expected. Since  $\nu_{LI}$  (and  $\omega_{LI}$ ) is larger than the fluorescence yield of the other two subshells—the more tightly a given shell or subshell is bound in an atom, the larger the fluorescence yield— $\bar{\omega}_L$  should be somewhat larger than  $\omega_{KL}$ . This prediction is confirmed by the results shown in Table III.

Two general conclusions can be drawn as a result of these experiments. (1) The early measurements of Lay are apparently accurate since they are in good agreement with the most recent determinations of fluorescence yields. (2) There remains a serious discrepancy between the present experiments and the work of Küstner and Arends,<sup>8</sup> Kinsey,<sup>11</sup> and Roos.<sup>9</sup> In the case of Küstner and Arends, the difficulty of calibrating gas-filled counters may be the cause of the difference. Inaccuracies in estimating the width of absorption edges may be the origin of the difference between the present measurements and Kinsey's estimates of  $L$ -shell fluorescence yields.

The authors gratefully acknowledge the help of Arnold Kirkwoog and Edward Zaharis during the course of this work.